Article

Study of the Optimization of Rail Pressure Characteristics in the High-Pressure Common Rail Injection System for Diesel Engines Based on the Response Surface Methodology

Ruichuan Li [1,2]**, Wentao Yuan** [1]**, Jikang Xu** [3,]***** **, Lin Wang** [4,]*****, **Feng Chi** [5]**, Yong Wang** [5]**, Shuqiang Liu** [5]**, Jianghai Lin** [2]**, Qingguang Zhang** [1] **and Lanzheng Chen** [1]

1   School of Mechanical Engineering, Qilu University of Technology (Shandong Academy of Sciences), Jinan 250353, China; liruichuan2021@163.com (R.L.); 18603842732@163.com (W.Y.)
2   Shandong Institute of Mechanical Design and Research, Jinan 250031, China
3   School of Transportation, Shandong University of Science and Technology, Qingdao 266590, China
4   State Key Laboratory of Intelligent Agricultural Power Equipment, Luoyang 471000, China
5   Shandong Lingong Construction Machinery Co., Ltd., Linyi 276000, China; feng.chi@sdlg.com.cn (F.C.)
*   Correspondence: xujikang121@163.com (J.X.); 15238486305@163.com (L.W.)

Abstract: This paper establishes a mathematical model of the high-pressure common rail injection system used in diesel engines according to the parameters of its key components, and AMESim 2020 software was used to establish a simulation model of the common rail injection system used in diesel engines. The simulation model mainly includes a high-pressure oil pump model, a common rail pipe model, and a model of four injectors. This paper also describes an experimental analysis of the accuracy of the established simulation model. Through a simulation analysis of the system rail's pressure fluctuation and pressure characteristics, it was concluded that the length of the common rail pipe, the diameter of the common rail pipe, and the inner diameter of the high-pressure fuel pipes are important influencing parameters for the rail pressure characteristics of the system. In this study, according to the original common rail pipe and high-pressure fuel pipe model, a response surface methodology was used to optimize and analyze the parameters of the common rail pipe and high-pressure fuel pipes, and the optimal size parameters for the common rail pipe and high-pressure fuel pipes were obtained with the minimum rail pressure fluctuations and the average rail pressure setpoint. After the optimization, the pressure for the common rail pipe of the high-pressure common rail system was increased by 0.82%, the pressure fluctuation was reduced by 21.66%, the injection pressure was increased by 1.15%, the single injection volume was increased by 0.86%, and its fuel injection characteristics were significantly improved.

Keywords: diesel engines; high-pressure common rail; average rail pressure; average rail pressure fluctuation; response surface methodology

1. Introduction

With the continuous development of technology and the industrial level, diesel engines are being widely used in fields such as transportation, industry, and national defense technology due to advantages such as wide power range, high thermal efficiency, high safety, and large output torque [1–3]. With the increase in the number of internal combustion engines, such as diesel engines, the environmental pollution caused by them has gradually become a serious problem. At the same time, people's awareness of environmental protection has gradually increased, and the requirements for energy conservation and emission reductions for diesel engines have also increased, and stricter emission regulations have been issued [4,5].

In contrast to the traditional diesel engine fuel injection system, high-pressure common rail injection systems are widely used in various diesel engines because of their capacity for

the flexible adjustment of injection pressure, independent and flexible control of injection timing and quantity, and high control accuracy, and they can effectively improve the economic aspects, power, and emissions of diesel engines [6–10]. In high-pressure common rail systems for diesel engines, the common rail pipe [11,12], as an important energy storage element in the common rail system, has an important impact on the control of the rail pressure fluctuations, common rail pressure and fuel injection quantity. Rail pressure fluctuations and common rail pressure not only determine the fuel injection pressure and injection quantity but are also the main measurement parameters of the system. The fluctuations in and magnitude of common rail pressure directly affect the performance of diesel engines during startup, idle times, and acceleration. Thus, one of the key measures to improve diesel engine performance is to suppress the fluctuations in rail pressure and increase the pressure for the common rail pipe. Therefore, many scholars have conducted studies on how to effectively suppress pressure fluctuations in the common rail pipe and improve the fuel pressure inside the common rail pipe.

Li et al. [13] analyzed the rail pressure change process caused by the injector of high pressure in the common rail injection system when injecting fuel. The test showed that the rail pressure drop rate was monotonically positively correlated with the fuel injection volume, and the total rail pressure drop caused by fuel injection was also positively correlated with the total fuel injection volume and independent of the number of injections.

Nie et al. [14] established a simulation model for a common rail system composed of two common rail pipes and conducted research on the pressure fluctuation characteristics in the rail cavity. The test showed that the length and diameter of the connecting pipe between the two common rail pipes had a greater impact on the pressure fluctuations after connecting the pipe and a smaller impact before connecting the pipe.

Zhao [15] studied the pressure fluctuation characteristics of the common rail pipe in a common rail system. Starting from the two processes of fuel supply and fuel injection, he studied the influence of the key parameters of the two processes on the rail pressure fluctuations and summarized the influence of the structure parameters of the fuel supply pump and fuel injector of the system on the superposition process for the pressure fluctuations in the rail.

Xiao [16] conducted research on the fuel injection characteristics of a vehicle high-pressure common rail system. In order to obtain the weight of the influence of each parameter on the rail pressure fluctuation characteristics, he conducted an orthogonal test analysis of the parameters of the key components of the common rail system. The experimental results showed that the inner diameter and the length of the common rail pipe had the greatest impacts on rail pressure fluctuations, and the parameters affecting rail pressure fluctuations were optimized, resulting in a 49.6% reduction in the average fluctuations in the system rail pressure.

Wang [17] studied the influence of the common rail pipe diameter, plunger diameter, high-pressure tubing length, and other geometric parameters on the fuel injection characteristics and the common rail pressure fluctuations in a certain type of electronically controlled, high-pressure, common rail fuel injection system for diesel engines and screened out several parameters with a greater influence on the system based on the experimental design and data-processing methods. He used a Pareto genetic optimization algorithm to improve the fuel injection pressure and reduce the rail pressure fluctuations as the objective function, optimized and analyzed the system, and finally obtained a new type of common rail pipe structure. This structure can effectively suppress the rail pressure fluctuations and improve the stability of the system's fuel injection performance.

Valery [18] took the characteristics of high-pressure fuel-pressure fluctuations in the fuel rail as the research object and analyzed the reasons for the formation of pressure fluctuations in the fuel rail, the fluctuation patterns, and the influence of geometric parameters on pressure fluctuations. The experiment showed that the length and diameter of the common rail pipe can affect its pressure fluctuations, and the longer the length and diameter of the common rail pipe, the smaller the amplitude of the rail pressure fluctuations.

At present, scholars' research on the common rail pipe and high-pressure oil pipes of a high-pressure common rail system mainly focuses on the following aspects: conducting relevant research on the regularity and characteristics of rail pressure changes; improving the control strategy of the rail pressure and injection pressure of common rail systems to improve their performance; design a new type of common rail pipe structure to suppress rail pressure fluctuations and other aspects more effectively. However, there is relatively little research on the optimization design of key structural parameters, such as common rail pipes and high-pressure oil pipes, that affect the rail pressure fluctuations, common rail pressure, and fuel injection characteristics of the common rail system. Therefore, this paper is based on the established AMESim simulation model of the diesel engine common rail fuel injection system, the average rail pressure characteristics and rail pressure fluctuation characteristics of the system are obtained. With the minimum and maximum rail pressure fluctuations as the goal, the response surface methodology is used to optimize the design and analysis of the common rail pipe and high-pressure fuel pipes.

2. Mathematical Mode of the High-Pressure Common Rail Injection System (HPCRIS) for Diesel Engines

This section first introduces the working principle of HPCRIS and then establishes mathematical models, including a high-pressure fuel pump, common rail pipe, and injector, based on continuity equation, momentum theorem, and Newton's law of motion.

2.1. Description of the HPCRIS

As a complex nonlinear system under multi-physical couplings, the HPCRIS contains many physical fields, such as mechanical, mechanical and electromagnetic fields. The internal flow field characteristics of the system cannot be completely obtained by a single test or piece of research, but the establishment of a numerical simulation model can effectively observe the changes in the internal flow field of the HPCRIS. The HPCRIS [19–22] mainly includes a high-pressure oil pump, common rail pipe, fuel injectors, electronic control unit ECU and other components. The framework is shown in Figure 1.
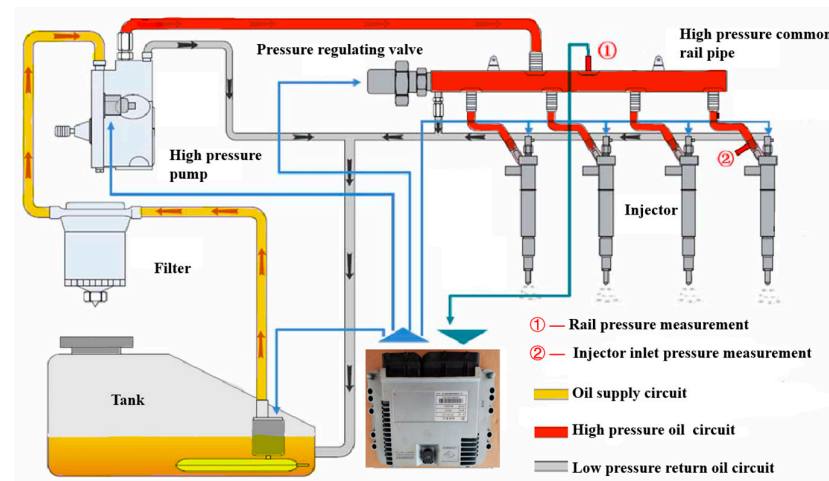
Figure 1. High-pressure common rail injection system.

Diesel oil is supplied from the fuel tank to the high-pressure fuel pump through a low-pressure fuel supply pump, which pressurizes the low-pressure fuel and delivers it to the common rail pipe. The main function of the common rail pipe is to store fuel and suppress fluctuations in rail pressure. A portion of the fuel within the common rail pipe is injected into the combustion chamber through the fuel injectors, while a small portion controls the injector needle valve and flows back to the fuel tank. The pressure sensor installed on the common rail pipe compares the actual rail pressure with the set value in the ECU. Subsequently, the ECU outputs a control signal to adjust the rail pressure to near

the set value. Serving as the core of the HPCRIS for diesel engines, the ECU determines the fuel pressure according to the optimal working state of the diesel engine by collecting various sensor signals.

2.2. Fuel Fluid Mathematical Model

The flow of fuel within the fuel pipes can be regarded as a one-dimensional compressible fluid flow in a circular pipe. Its continuity differential equation, motion differential equation, and fuel state equation [23] are as follows.

$$\frac{\partial \rho}{\partial t} + \rho \frac{\partial u}{\partial x} + \mu \frac{\partial \rho}{\partial x} = 0 \tag{1}$$

$$\frac{\partial u}{\partial t} + \mu \frac{\partial u}{\partial x} + \frac{1}{\rho} \frac{\partial}{\partial x} P + G = 0 \tag{2}$$

$$a^2 = \frac{\partial P}{\partial \rho} \tag{3}$$

where P is the pressure; ρ is the fuel density; μ is the flow rate; a is the propagation velocity of the pressure wave; G is the friction in the direction x per unit mass.

2.3. Mathematical Model of the High-Pressure Oil Pump

The high-pressure oil pump is the power component of the HPCRIS for diesel engines. It converts the mechanical energy of the prime mover into the pressure energy of the liquid to provide high-pressure, high-energy fuel for the common rail fuel injection system. The mathematical model diagram of the high-pressure oil pump is shown in Figure 2.
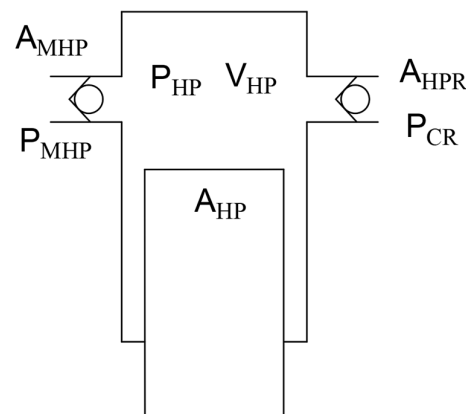
Figure 2. High-pressure oil pump model.

In Figure 2, A_{MHP} is the cross-sectional area at the oil inlet of the plunger cavity; P_{MHP} is the oil pressure in the proportional valve chamber; P_{HP} is the high-pressure oil pump plunger chamber pressure; V_{HP} is the volume of the high-pressure oil pump plunger cavity; A_{HPR} is the cross-sectional area from the outlet of the plunger chamber to the inlet of the common rail pipe; P_{CR} is the pressure of the common rail pipe.

This paper establishes mathematical formulas for the diesel oil flow rate based on the high-pressure oil pump model as follows [12,24,25].

The flow relationship in the plunger cavity of the high-pressure oil pump from time t to time $t + \Delta t$ is expressed as follows.

$$Q_{HP} = Q_{VHP} + Q_{HP \rightarrow CR} + Q_{MHP} + Q_{LHP} \tag{4}$$

where Q_{HP} is the geometric fuel supply; Q_{VHP} is the fuel compression flow caused by pressure changes in the plunger cavity of the high-pressure oil pump; $Q_{HP \rightarrow CR}$ is the flow

rate of the high-pressure oil pump plunger chamber flowing to the common rail pipe through the outlet check valve; Q_{MHP} is the flow rate of the inlet metering proportional valve to the plunger chamber; Q_{LHP} is the leakage flow rate of the high-pressure oil pump plunger cavity.

The geometric fuel supply Q_{HP} is expressed as follows.

$$Q_{HP} = A_{HP} u_{HP} \tag{5}$$

where μ_{HP} is the plunger speed; A_{HP} is the cross-sectional area of the plunger.

By organizing Formula (4), it can be concluded that.

$$\frac{V_{HP}}{E}\frac{dP_{HP}}{dt} = A_{HP} u_{HP} - \xi(\mu A_{HPR})\sqrt{\frac{2}{\rho}|P_{HP} - P_{CR}|} - \gamma(\mu A_{MHP})\sqrt{\frac{2}{\rho}|P_{HP} - P_{MHP}|} - \frac{\pi d_{HP}\delta_{HP}^3}{12\eta L_{HP}}(P_{HP} - P_O) \tag{6}$$

2.4. Mathematical Model of the High-Pressure Common Rail Pipe

The common rail pipe serves as the energy storage element in the HPCRIS for diesel engines. It plays the role of storing and delivering fuel and is mainly used to suppress the fluctuation in rail pressure. The common rail pipe can be simplified into a rectangular cuboid volume, and its main parameter is its volume. The three-dimensional model and simplified model of the high-pressure common rail pipe are shown in Figure 3.

(**a**) (**b**)
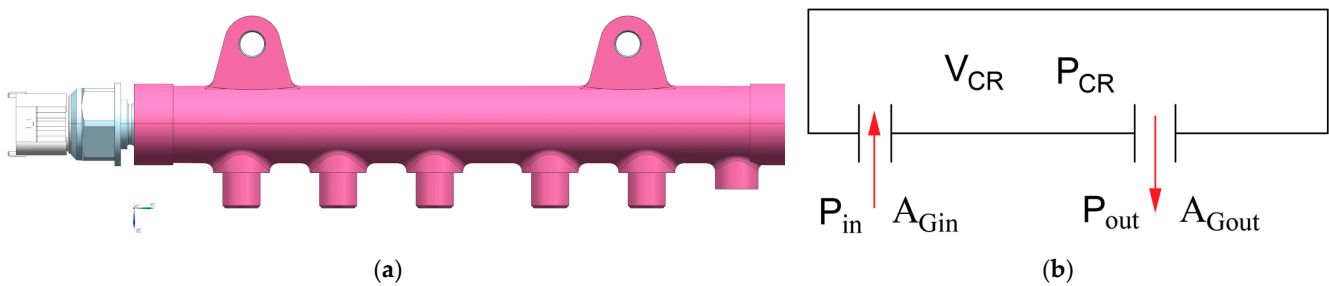
Figure 3. High-pressure common rail pipe model. (**a**) Three-dimensional model of the common rail pipe; (**b**) simplified model of the common rail pipe.

This paper establishes mathematical formulas for the diesel oil flow rate based on the high-pressure common rail pipe model as follows [24,26].

The flow relationship within the common rail pipe from time t to time $t + \Delta t$ is expressed as follows.

$$Q_{HP \to CR} = Q_{VCR} + Q_{CR \to OS} + Q_{CRK} + Q_{CRO} \tag{7}$$

The fuel compression rate caused by changes in rail pressure Q_{VCR} is expressed as follows.

$$Q_{VCR} = \frac{V_{CR}}{E}\frac{dP_{CR}}{dt} \tag{8}$$

where V_{CR} is the volume of the common rail pipe; P_{CR} is the pressure of the common rail pipe.

The flow rate of the common rail pipe to the fuel tank of fuel injectors $Q_{CR \to OS}$ is expressed as follows.

$$Q_{CR \to OS} = \kappa(\mu A_{CR \to OS})\sqrt{\frac{2}{\rho}|P_{CR} - P_{OS}|} \tag{9}$$

where $\mu A_{CR \to OS}$ is the effective flow area of the common rail pipe flowing to the fuel tank of the fuel injector; P_{OS} is the pressure in fuel injectors' sump; $\kappa = \begin{cases} 1, & if\ P_{CR} \geq P_{OS} \\ 0, & if\ P_{CR} < P_{OS} \end{cases}$.

The amount of fuel flowing from the common rail pipe to the control chamber of the fuel injector Q_{CRK} is expressed as follows.

$$Q_{CRK} = \zeta(\mu A_{CRK})\sqrt{\frac{2}{\rho}|P_{CR} - P_K|} \tag{10}$$

where μA_{CRK} is the effective flow area of the common rail pipe flow control chamber; P_K is the pressure of the fuel in the chamber; $\zeta = \begin{cases} 1, & if\ P_{CR} \geq P_K \\ 0, & if\ P_{CR} < P_K \end{cases}$.

The flow rate of the common rail pipe to the low-pressure oil passage Q_{CRO} is expressed as follows.

$$Q_{CRO} = \lambda(\mu A_o)\sqrt{\frac{2}{\rho}|P_{CR} - P_O|} \tag{11}$$

where μA_O is the effective flow area of the common rail pipe to the low-pressure oil passage; P_O is the pressure of fuel in the low-pressure fuel circuit; $\lambda = \begin{cases} 1, & if\ P_{CR} \geq P_O \\ 0, & if\ P_{CR} < P_O \end{cases}$.

The above formulas can be organized as follows.

$$\frac{V_{CR}}{E}\frac{dP_{CR}}{dt} = Q_{HP \to CR} - \kappa(\mu A_{CR \to OS})\sqrt{\frac{2}{\rho}|P_{CR} - P_{OS}|} - \zeta(\mu A_{CRK})\sqrt{\frac{2}{\rho}|P_{CR} - P_K|} - \lambda(\mu A_o)\sqrt{\frac{2}{\rho}|P_{CR} - P_o|} \tag{12}$$

2.5. Mathematical Model of Fuel Injectors

In order to simplify the model, the pressure loss and local pressure loss from the outlet of the common rail pipe to the inlet of the fuel injectors' hole are usually ignored. Consequently, the pressure at the high-pressure tubing end can be considered to be equal to the nozzle-end pressure. This paper establishes the mathematical formulas for the diesel oil flow rate of fuel injectors' mathematical model as follows [16,27].

2.5.1. Fuel Continuity Equation in the Control Chamber of the Fuel Injectors

From time t to time $t + \Delta t$, the fuel flow relationship within the control chamber of the fuel injectors is expressed as follows.

$$Q_{CRK} = Q_{KO} + Q_{KX} + Q_{KC} \tag{13}$$

where Q_{KO} is the flow from the control chamber to the return channel; Q_{KX} is the fuel leakage from control valve piston coupling; Q_{KC} is the fuel compression rate caused by changes in control chamber pressure.

By organizing Formula (13), it can be concluded that.

$$\frac{V_{KC}}{E}\frac{dP_{KC}}{dt} = \zeta(\mu A_{CRK})\sqrt{\frac{2}{\rho}|P_{CR} - P_K|} - \psi(\mu A_o)\sqrt{\frac{2}{\rho}|P_K - P_O|} - \frac{\pi d_K \delta_K^3}{12\eta L_K}(P_K - P_O) \tag{14}$$

2.5.2. Fuel Continuity Equation in the Fuel Tank of Fuel Injectors

From time t to time $t + \Delta t$, the flow relationship within fuel injectors' sump is expressed as follows.

$$Q_{CR \to OS} = Q_{ZF} + Q_{OS \to NY} + Q_{NVL} + Q_{OSR} \tag{15}$$

where $Q_{CR \to OS}$ is the flow rate from the common rail pipe to the oil tank; Q_{ZF} is the flow change caused by needle lift changes; $Q_{CR \to NY}$ is the flow rate from fuel injectors' sump to the nozzle pressure chamber; Q_{NVL} is the leakage of needle valve components; Q_{OSR} is the fuel compression rate caused by pressure changes in the oil tank.

2.5.3. Fuel Continuity Equation in Fuel Injectors' Pressure Chamber

From time t to time $t + \Delta t$, the flow rate within the fuel injectors' pressure chamber is expressed as follows.

$$Q_{OS \to NY} = Q_{NY \to BS} + Q_{NYR} \tag{16}$$

where $Q_{NY \to BS}$ is the flow rate from the pressure chamber to combustion chamber; Q_{NYR} is the fuel compression rate caused by pressure changes in the oil tank.

3. Simulation Model of the HPCRIS for Diesel Engines

In this paper, the AMESim software is used to establish the hydraulic simulation model of the HPCRIS for diesel engines. Considering the complexity and precision of the HPCRIS, the following assumptions are made for the simulation model.

(1) The diesel oil flow through the HPCRIS pipe is regarded as a compressible, one-dimensional, unsteady laminar flow.
(2) During the operation of fuel injectors, it is assumed that the temperature of the HPCRIS remains constant.
(3) Fuel gravity and heat transfer generated during system operation are neglected.
(4) It is assumed that the density and elastic modulus of fuel are only related to the rail pressure, and assumed that the viscosity of fuel is considered to remain constant.
(5) It is assumed that the fuel pressure and density at the same time are the same in all parts of the same volume chamber.

The simulation model of the common rail fuel injection system established in this paper is shown in Figure 4. The model mainly includes four injectors, a low-pressure fuel pump and a high-pressure fuel pump, a common rail pipe, and a controller.

High-pressure oil pump

ECU

High-pressure common rail pipe

High-pressure fuel injectors
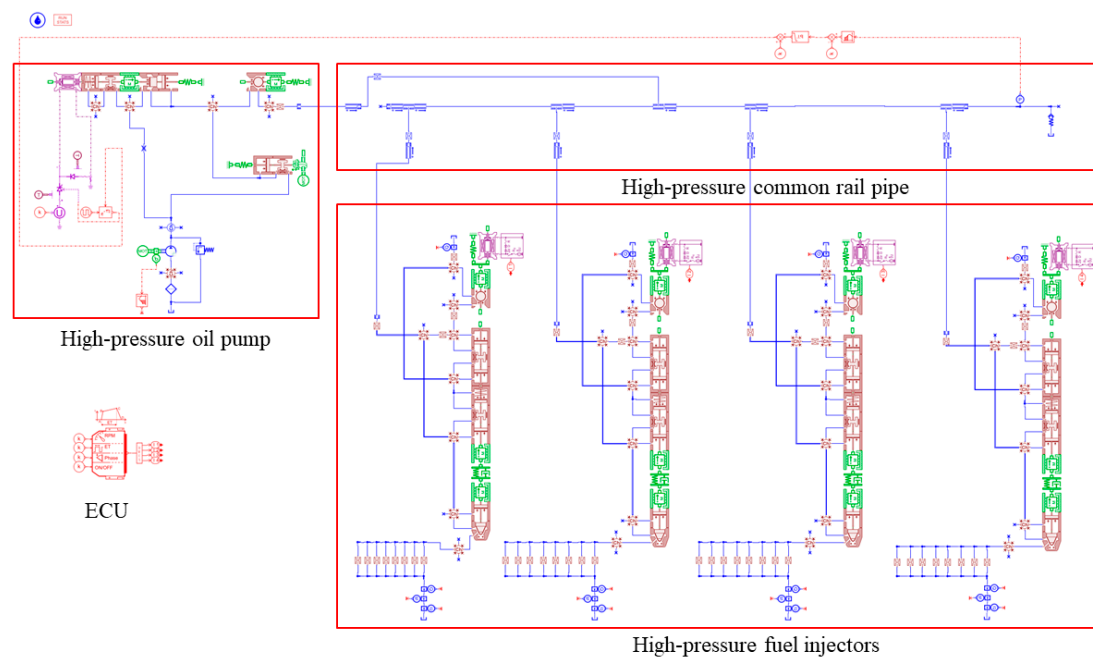
Figure 4. Simulation diagram of the HPCRIS for diesel engines.

The important key parameters of this simulation model are shown in Table 1.

In order to verify the accuracy of building the AMESim model of the HPCRIS, the common rail pressure is set to 100 MPa, 150 MPa and 200 MPa, and the injection pulse width is set to 0.25–2 ms. According to Figure 5, it can be concluded that the fuel injection errors of the test and simulation under different injection pulse widths are less than 5%, and the accuracy of the established model is high enough to meet the experimental requirements.

Table 1. Key parameters of simulation model.

Module Name	Parameter	Parameter Value
diesel	Diesel density	835 kg/m^3
	Diesel temperature	60 °C
High-pressure oil pump	Oil pump speed	2000 r/min
	Plunger length	35 mm
	Plunger diameter	8 mm
Common rail pipe	Outer diameter of the common rail pipe	30 mm
	Length of the common rail pipe	248 mm
	Inner diameter of the common rail pipe	7 mm
High-pressure oil pipes	Diameter of high-pressure oil pipes	3 mm
	Injection time	1 ms
Injectors	Number of orifices	8
	Equivalent orifice diameter	0.16 mm
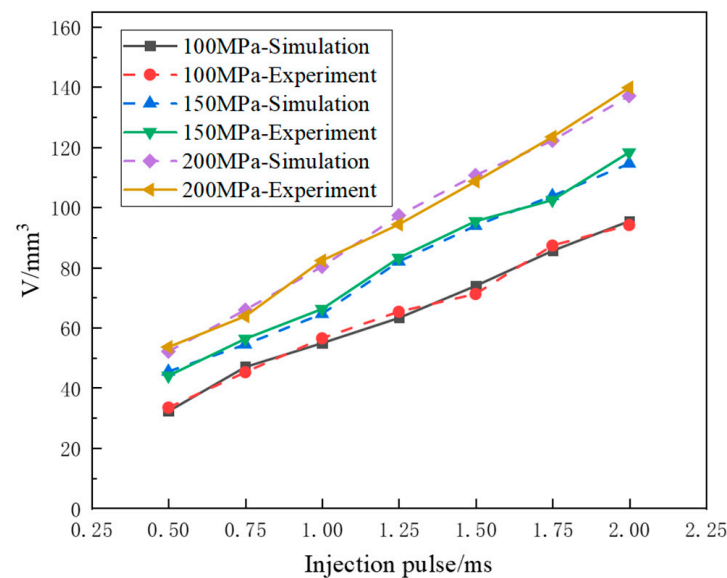
Figure 5. Comparison results of experimental and simulated fuel injection quantities.

4. Single Factor Parameter Analysis

The research objects of this paper are the common rail pipe of ER2090001 and high-pressure oil pipes of EG3090001 in the four high-pressure injectors of a common rail system of a company. The main parameters are shown in Table 1. Through a series of simulation studies on the key components of a common rail pipe and high-pressure oil pipes, it is found that the parameters of common rail pipe length *L*, and diameter *D*, and high-pressure fuel pipes with diameter *R*, have an important impact on the injection characteristics of the HPCRIS for diesel engines.

4.1. Effect of Common Rail Pipe Length L Change on Injection Characteristics

Under the condition that the diameter of the high-pressure oil pipe remains unchanged by 3 mm, the changes in average rail pressure, rail pressure fluctuatiosn, injection pressure and injection quantity under the HPCRIS simulation model are shown in Figure 6. According to Figure 6a, when 186 mm < *L* < 496 mm, with the increase in *L*, the average rail pressure of the common rail pipe slowly increases and gradually tends to stabilize. According to Figure 6b, it can be seen that as *L* increases, the rate of decrease in the average orbital pressure wave momentum decreases.
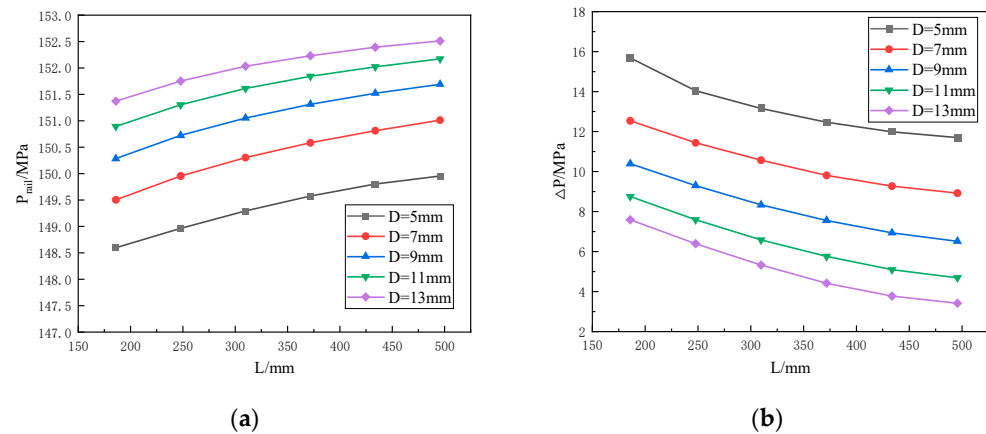
Figure 6. The impact of *L* changes on injection characteristics. (**a**) Average rail pressure; (**b**) average rail pressure fluctuations.

4.2. Effect of Common Rail Pipe Diameter D Changes on Injection Characteristics

In this paper, under the condition that the inner diameter of the high-pressure fuel pipes *R* = 3 mm is unchanged, the common rail pipe diameter of 5 mm < *D* < 13 mm is selected for simulation research. The injection characteristics of the simulation model of the HPCRIS are shown in Figure 7. The average rail pressure increases with the increase in *D*, while the fluctuations in average rail pressure decrease with the increase in *D*. Compared with the influence of *L* and *R* on the injection characteristics of the HPCRIS, the average rail pressure increase rate and average rail pressure fluctuation decrease rate under the *D* parameter are both the largest, which indicates that the diameter of the common rail pipe *D* has the most significant influence on both rail pressure and rail pressure fluctuations.
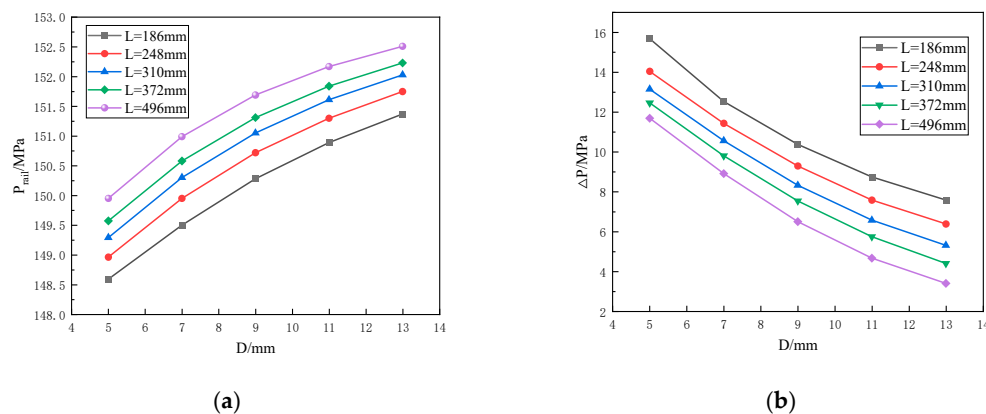
Figure 7. The impact of *D* changes on injection characteristics. (**a**) Average rail pressure; (**b**) average rail pressure fluctuations.

4.3. Effect of Diameter R Variations in High-Pressure Oil Pipes on Injection Characteristics

In the paper, under the condition that the length of the common rail pipe is 248 mm, the diameters of the high-pressure fuel pipes are 2 mm < *R* < 4 mm for simulation research. The fuel injection characteristics of the simulation model of the HPCRIS are shown in Figure 8. The average rail pressure increases with the increase in *R*, and the fluctuations in average rail pressure decrease with the increase in *R*. Additionally, the influence of high-pressure oil pipes' diameter *R* on rail pressure and rail pressure fluctuations is smaller than the influence of *L* and *D* parameters on rail pressure fluctuations.

(**a**)　　　　　　　　　　　　　　　　　　　　　　　(**b**)
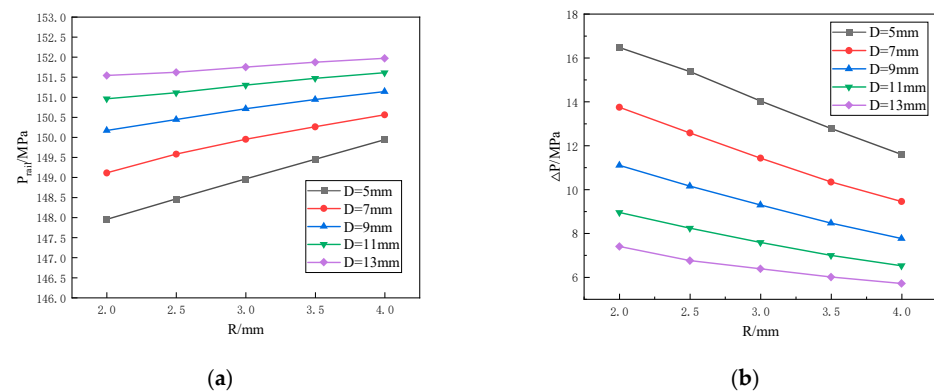
Figure 8. The impact of *R* changes on injection characteristics. (**a**) Average rail pressure; (**b**) average rail pressure fluctuations.

5. Optimization of Parameters for the Common Rail Pipe and High-Pressure Oil Pipes

5.1. Selection of Response Surface Methodology (RSM) Design Method and Variables

Based on the above research on the injection characteristics of *L*, *D* and *R* parameters, to optimize the fuel injection characteristics of the HPCRIS for diesel engines, the response surface methodology (RSM) will be used to optimize the common rail pipe pressure and the common rail pipe pressure fluctuation characteristics. Response surface methodology [17,28–31] searches for the best combination of independent variables by analyzing the relationship between target variables and independent variables through optimization methods based on statistical principles, and is used to optimize complex functions with multiple independent variables. RSM also encompasses regression design, which further enhances its ability to analyze and model the relationship between variables. Central composite design (CCD) and Box Behnken design (BBD) are commonly used in the response surface methodology. Due to the good approximation of CCD to response surfaces, which can improve the accuracy of optimization results and achieve a better surface approximation performance, this paper uses CCD design experiments to generate samples. This paper selects 15 samples in a three-dimensional space, including 1 center point, 6 axis points, and 8 diagonal points.

From the above analysis, it can be seen that the main structural parameters that affect the pressure fluctuations and average pressure of the common rail pipe are the length *L* of the common rail pipe, the diameter *D* of the common rail pipe, and the diameter *R* of the high-pressure fuel pipe between the common rail pipe and the fuel injector connection. Therefore, *L*, *D*, and *R* are selected as design variables in this paper. The range of values for each design variable is shown in Table 2.

Table 2. Design variable value range.

Design Variable/mm	Low Level (−)	High Level (+)
Length of common rail pipe *L*	186	496
Diameter *D* of common rail pipe	7	13
Diameter *R* of high-pressure pipe	2	4

The samples and corresponding simulation results generated using the CCD design in this paper are shown in Table 3.

Table 3. Samples and test results.

Serial Number	*L*/mm	*D*/mm	*R*/mm	Average Rail Pressure P_{rail}/MPa	Average Rail Pressure Fluctuation ΔP/MPa
1	186	5	4	149.74	12.25
2	341	9	3	151.19	7.76
3	496	13	4	152.62	3.31

Table 3. *Cont.*

Serial Number	L/mm	D/mm	R/mm	Average Rail Pressure P_{rail}/MPa	Average Rail Pressure Fluctuation ΔP/MPa
4	341	14.2643	3	152.33	4.21
5	341	9	4.31607	151.61	6.63
6	496	5	4	150.62	9.53
7	137.009	9	3	149.85	12.05
8	341	9	1.68393	150.83	9.99
9	186	13	2	151.04	8.67
10	496	5	2	149.23	14.37
11	186	13	4	151.66	6.52
12	496	13	2	152.45	3.97
13	341	3.7357	3	148.66	15.11
14	544.991	9	3	151.81	5.88
15	186	5	2	147.36	17.74

5.1.1. Analysis of the Average Pressure P_{rail} Test for the Common Rail Pipe

According to the simulation test results in Table 3, the polynomial regression model can be obtained by fitting the average pressure of the common rail pipe with the three structural parameters L, D and R through the Design Expert 13 software. The relationship is expressed as follows.

$$P_{rail} = 138.30987 + 0.014484L + 1.10127D + 1.633387R - 0.000077LD$$
$$-0.001161LR - 0.093125DR - 0.00000876476L^2 - 0.025249D^2 + 0.014593R^2 \tag{17}$$

Table 4 shows the effectiveness analysis of the P_{rail} model for the average pressure of common rail pipes. According to the table, the correlation coefficient R^2 of the average pressure P_{rail} test model for a common rail pipe is 0.9924; this is required, for engineering tests, to be above 0.9. This indicates that the model has a good fitting degree, and the error is within a reasonable range. The signal-to-noise ratio Adeq Precision of this model is 46.4783, which is much greater than 4, indicating that the model has good resolution. In addition, the coefficient of variation C.V. is 0.1045%, indicating that the total variation in the model's response value is only 0.1045%, indicating high model accuracy.

Table 4. Effectiveness analysis of the average rail pressure P_{rail} model for the common rail pipe.

Category	Numerical Value
R^2	0.9924
Adj R^2	0.9856
Pre R^2	0.9937
Adeq precision	46.4783
C.V.	0.1045

Figure 9 shows the residual analysis of the average rail pressure P_{rail} model. According to Figure 9a, all residuals are evenly distributed near the straight line, with a good degree of linearization, indicating that the average rail pressure model of common rail pipe conforms to normal distribution. According to Figure 9b, the average pressure model is mostly distributed between −4.14579 and 4.14579. According to the distribution of the residual and operating number in Figure 9c, the average pressure residual of the common rail pipe is uniformly distributed above and below the 0-point coordinate axis, with a small deviation in the range of fluctuations. The residual distribution of the model meets the expected value. According to Figure 9d, the actual average pressure of the common rail pipe is uniformly distributed near the predicted regression line, and the error between the predicted value and the actual value of the model is very small, indicating that the stability and accuracy of the model are high.

(**a**)

(**b**)

(**c**)

(**d**)
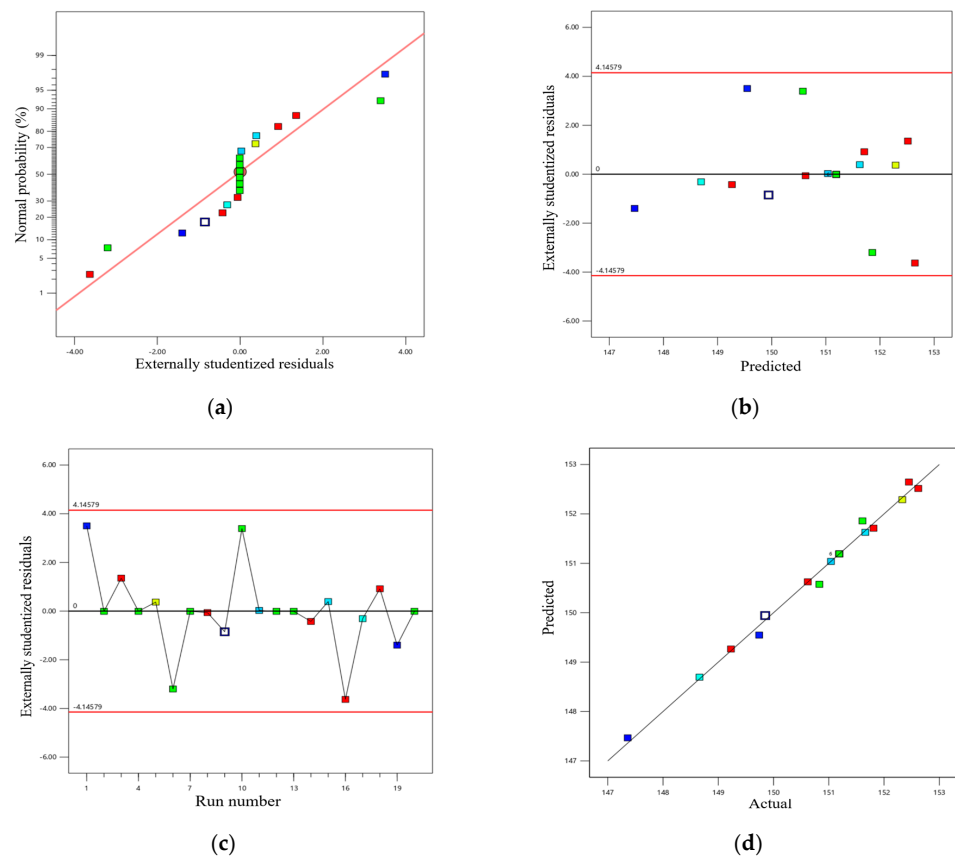
Figure 9. Analysis of average rail pressure P_{rail} residual. (**a**) Stable residual value; (**b**) residual and predicted value; (**c**) residuals and runing number; (**d**) predicted and actual value.

5.1.2. Analysis of the Rail Pressure Fluctuation ΔP Test for the Common Rail Pipe

According to the simulation test results in Table 3, a polynomial regression model can be obtained by fitting the average rail pressure fluctuations ΔP in the common rail pipe with the three structural parameters L, D and R, and the relationship is expressed as follows:

$$\Delta P = 42.36065 - 0.031008L - 2.69053D - 5.49296R - 0.000367LD$$
$$+ 0.001726LR + 0.235DR + 0.000024L^2 + 0.061813D^2 + 0.209592R^2 \tag{18}$$

Table 5 shows the effectiveness analysis of the ΔP model for pressure fluctuations in the common rail pipe. These were obtained in the same way as the above analysis. The correlation coefficient R^2 of the common rail pipe rail pressure fluctuation test model is 0.9945, indicating that the model fits well. The predicted correlation coefficient Pre R^2 is 0.9895, and the difference between this and the adjusted correlation coefficient Adj R^2 is less than 0.2, indicating that the model has a high prediction accuracy. The signal-to-noise ratio Adeq precision of the common rail pressure fluctuation model is 54.0104, indicating that the model has good resolution ability. In addition, the coefficient of variation C.V. of the model is 4.42%, which is less than 5%, indicating that the total variation in the response value of the model is only 4.42%, and the model accuracy is relatively high.

Table 5. Effectiveness analysis of rail pressure fluctuation ΔP model.

Category	Numerical Value
R^2	0.9945
Adj R^2	0.9895
Pre R^2	0.9560
Adeq precision	54.0104
C.V.	4.42

    Figure 10 below shows the residual analysis of the ΔP model for the average pressure fluctuations of the common rail pipe. Figure 10a shows that the residuals are uniformly distributed near the straight line, with a good degree of linearization. Figure 10b shows that the average pressure fluctuation model is generally distributed between −4.14579 and 4.14579. Figure 10c shows that the average rail pressure fluctuation residual of the common rail pipe is uniformly distributed above and below the 0-point coordinate axis, and the deviation range of the fluctuation is relatively small. The residual distribution of the model meets the expected value. Figure 10d shows that the average pressure fluctuation value of the common rail pipe is uniformly distributed near the predicted regression line, and the model has a small error between the predicted value and the actual value. The stability and accuracy of the model are relatively high.
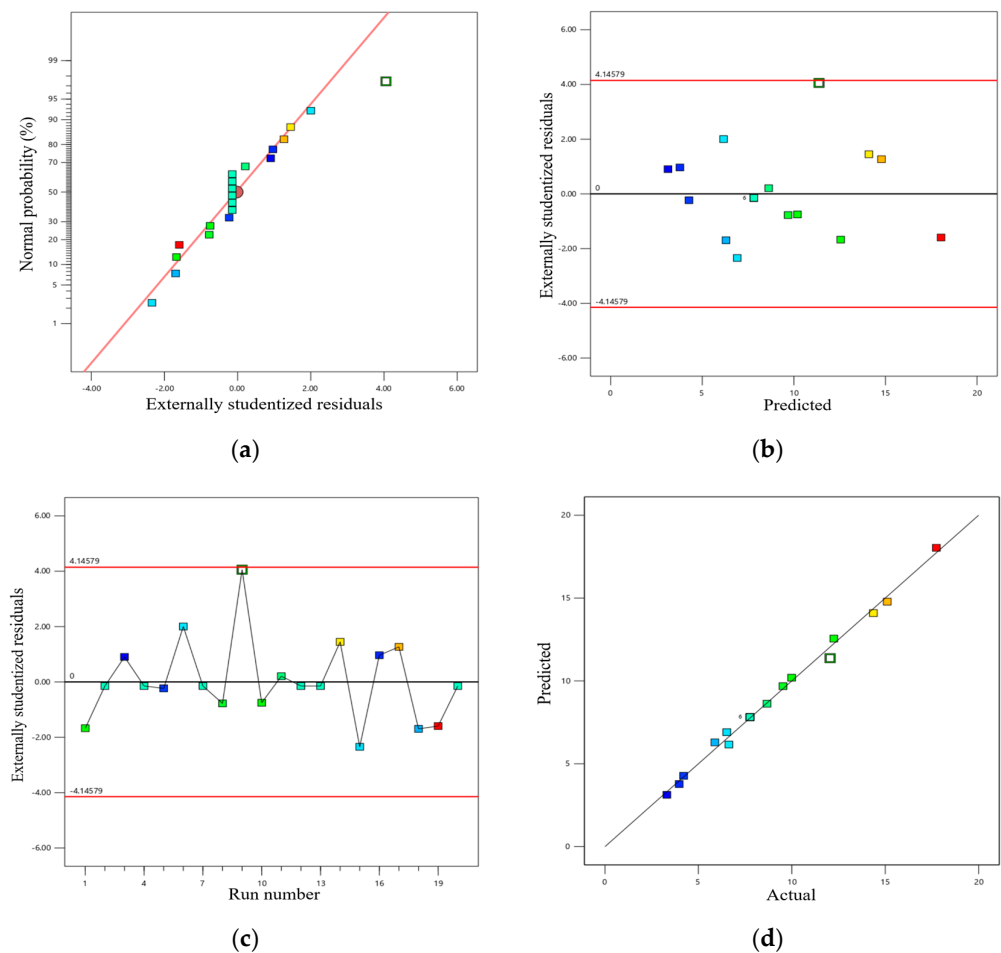
Figure 10. Analysis of average rail pressure ΔP residual. (**a**) Stable residual value; (**b**) residual and predicted value; (**c**) residuals and running number; (**d**) predicted and actual value.

5.2. Analysis of Variance

5.2.1. Analysis of Variance in the Average Rail Pressure P_{rail} for the Common Rail Pipe

    The variance in the polynomial model regarding the average rail pressure of the common rail pipe is shown in Table 6. When the *p*-value of a parameter in the model is less than 0.05, this indicates that the parameter is significant for the response. When the *p*-value is greater than 0.05, this indicates that the parameter is not significant for the response. According to Table 6, the *p*-values of parameters *L*, *D*, *R*, *LR*, *DR*, L^2, and D^2 are all less than 0.005, indicating that these parameters have a significant response to the model. The F value of the model is 145.03, indicating that the model is significant. The larger the F value of a certain parameter in the model, the more significant the influence of this parameter on

the average rail pressure model of the common rail pipe. Therefore, the weights of each influence are D, L, R, D^2, DR, L^2, LR, LD, and R^2.

Table 6. Analysis of variance in the average rail pressure P_{rail}.

Source of Variance	Mean Square	Freedom	F	p
model	32.41	9	145.03	<0.0001
L	5.17	1	208.28	<0.0001
D	21.36	1	860.50	<0.0001
R	2.72	1	109.65	<0.0001
LD	0.0181	1	0.7270	0.4138
LR	0.2592	1	10.44	0.0090
DR	1.11	1	44.71	<0.0001
L^2	0.3090	1	12.44	0.0055
D^2	1.14	1	45.80	<0.0001
R^2	0.0015	1	0.0598	0.8118
pure error	0.0000	10	0.0000	
comprehensive	32.65	19		

5.2.2. Analysis of Variance in the Average Pressure Fluctuation ΔP in the Common Rail Pipe

The variance in the polynomial model for the average rail pressure fluctuations in the common rail pipe is shown in Table 7. According to the table, the p-values of parameters L, D, R, DR, L^2, and D^2 are all less than 0.005, indicating that these parameters are important influencing factors for the model. The F-value of the model is 179.17, indicating that the model is significant.

Table 7. Analysis of variance in the average rail pressure fluctuations ΔP.

Source of Variance	Mean Square	Freedom	F	p
model	273.10	9	199.17	<0.0001
L	42.68	1	280.15	<0.0001
D	182.70	1	1199.16	<0.0001
R	26.90	1	176.59	<0.0001
LD	0.4140	1	2.72	0.1303
LR	0.5725	1	3.76	0.0813
DR	7.07	1	46.40	<0.0001
L^2	2.41	1	15.80	0.0026
D^2	6.82	1	44.74	<0.0001
R^2	0.3061	1	2.01	0.1868
pure error	0.0000	10	0.0000	
comprehensive	274.62	19		

5.3. Analysis of the Impact of Interaction Parameter Factors

5.3.1. Analysis of the Influence of Interaction Parameter Factors on the Average Rail Pressure P_{rail}

The influence of the interaction factor between L and D parameters on the average rail pressure P_{rail} is shown in Figure 11a; when 186 mm < L < 496 mm, the average rail pressure of the common rail pipe increases with the increase in L. The analysis of the interaction factor between L and R on the average rail pressure is shown in Figure 11b; when R is fixed, the average rail pressure increases with the increase in L, and an appropriate increase in R can be conducive to increasing the average rail pressure. The analysis of the interaction factor between D and R on the average rail pressure is shown in Figure 11c. When D is a constant value, increasing R is beneficial to increasing the average rail pressure. As R increases, the average rail pressure eventually tends to stabilize to an equal value. According to the overall analysis in Figure 11, it can be seen that as L, D, and R increase,

the slope of the average rail pressure increase gradually decreases, and the rail pressure increase gradually stabilizes.
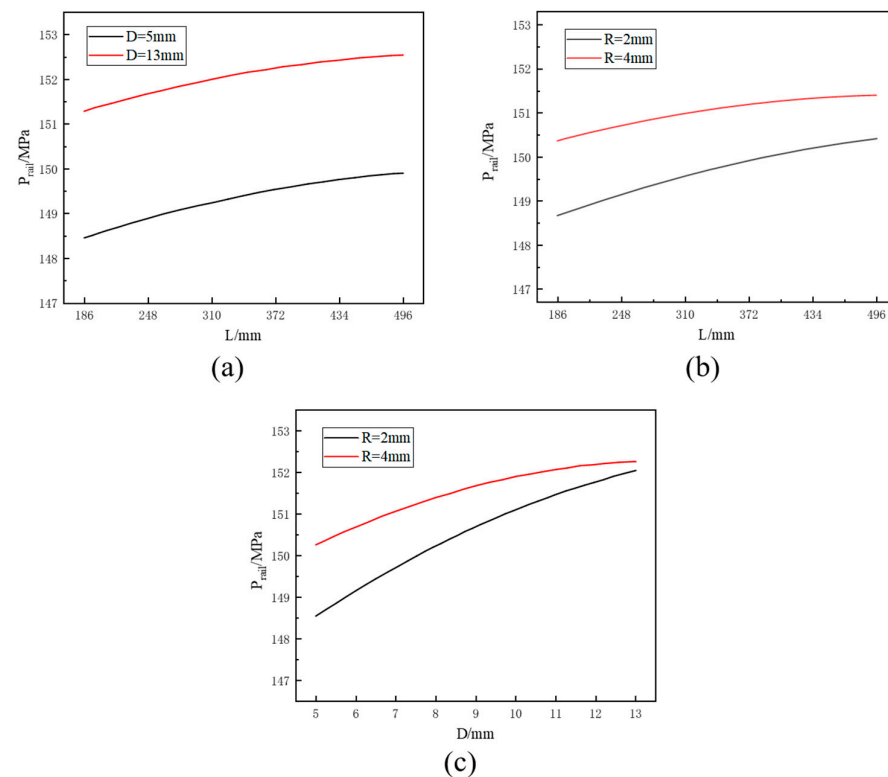
Figure 11. Analysis of average rail pressure P_{rail} interaction factors. (**a**) L and D interaction; (**b**) L and R interaction; (**c**) D and R interaction.

5.3.2. Analysis of the Influence of Interactive Parameters on the Average Rail Pressure Fluctuations ΔP

The interactive effect of parameter factors L and D on the average rail pressure fluctuations ΔP is shown in Figure 12a. When D remains constant, the average rail pressure fluctuation decreases with the increase in L. An appropriate increase in L can effectively suppress the rail pressure fluctuations, but when L is large, the rate of decline in rail pressure fluctuations gradually tends to flatten. The interactive effect of the L and D parameter factors on the average rail pressure fluctuations ΔP is shown in Figure 12b. When 186 mm $< L <$ 496 mm, the rail pressure fluctuations gradually decrease with the increase in R. An appropriate increase in L is beneficial o effectively suppressing the rail pressure fluctuations. The interactive effect of the D and R parameter factors on the average rail pressure fluctuations ΔP is shown in Figure 12c. When R is a fixed value, the rate of rail pressure fluctuation decreases with the increase in D is greater than the rate of rail pressure fluctuation decreases under the influence of L and R parameters, indicating that D has the most significant impact on the rail pressure fluctuations.

5.4. Response Surface Optimization Analysis

5.4.1. Response Surface Optimization Analysis of the Average Rail Pressure P_{rail} in the Common Rail Pipe

The three-dimensional response surface is established to further explore the influence of each design parameter variable on the average fuel pressure of the common rail pipe, as shown in following figures. The inclination of the surface represents the degree of influence of the factor on the average fuel pressure, with a higher inclination indicating a greater impact of the factor on the average rail pressure, and a darker red color indicating the larger average rail pressure value.
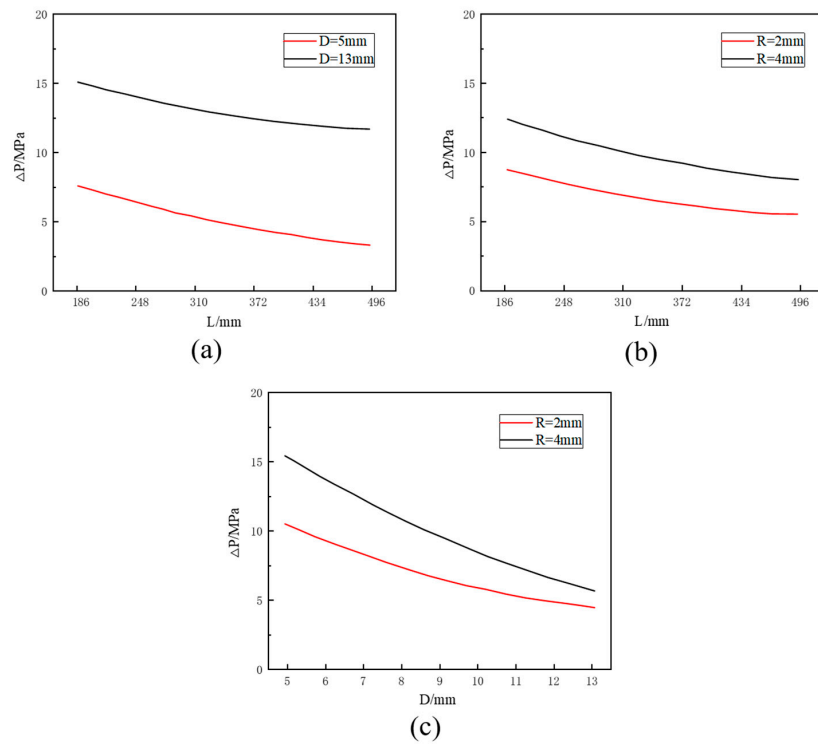
Figure 12. Analysis of average rail pressure fluctuation ΔP interaction factors. (**a**) L and D interaction; (**b**) L and R interaction; (**c**) D and R interaction.

In Figure 13a contour plane, it can be concluded that the contours of L and D have obvious changes, and the density of the contour distribution of D is greater than that of L, indicating that the influence of D on the average rail pressure is greater than that of L. As shown in Figure 13b, L and D have a significant impact on the average rail pressure of the common rail pipe. The larger values of the average rail pressure are distributed in the upper right area of the response surface, which is the area with a larger L and D.
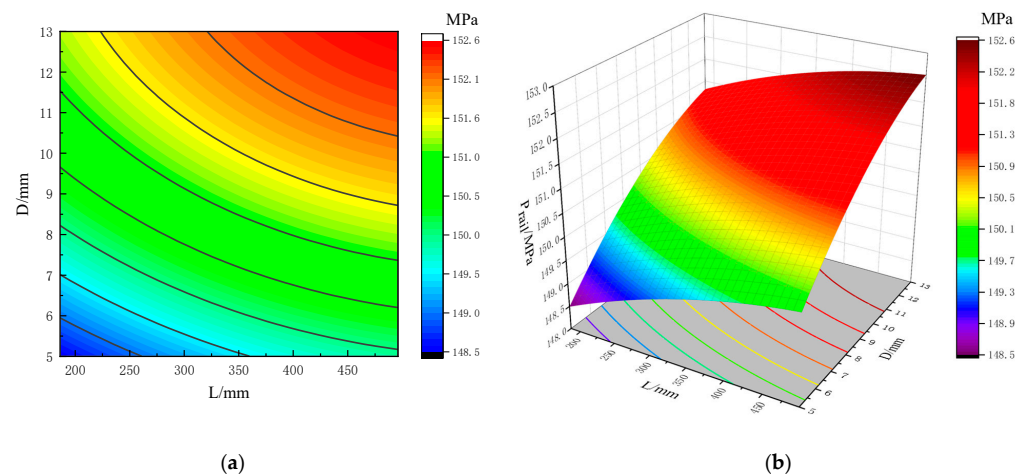
Figure 13. Interaction response of design variables L and D with average rail pressure. (**a**) Contour plane of L and D factors; (**b**) response surface of L and D factors.

As shown in Figure 14a contour plane, the density of the contour distribution of L is greater than that of R, indicating that the influence of L on the average rail pressure is greater than that of R. As shown in Figure 14b, there is a significant change in the inclination of the surface in the direction of the L change, while the inclination of the surface in the

direction of R change is relatively small, meaning that L has a greater impact on the average rail pressure and R has a smaller impact on the average rail pressure value. The maximum rail pressure is distributed in the areas with a larger L and R, which are on the upper right side of the surface.

(a) (b)
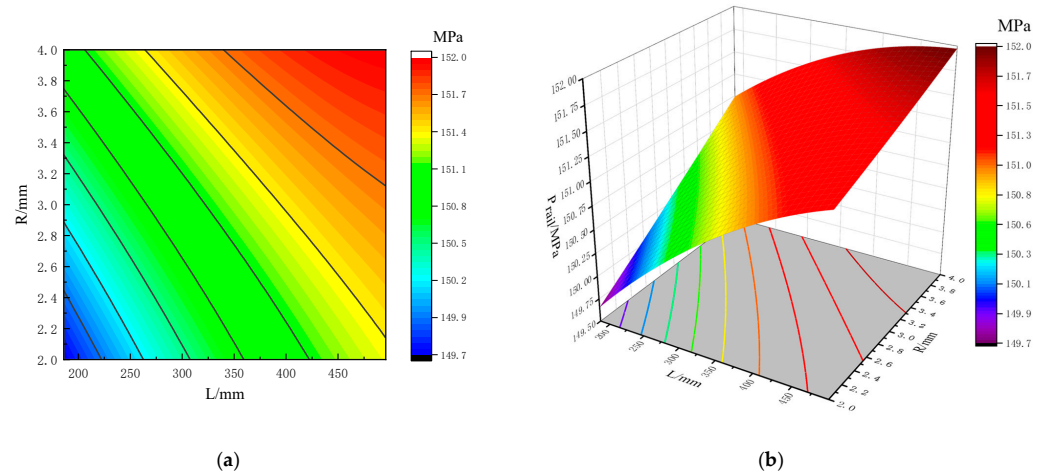
Figure 14. Interaction response of design variables L and R with average rail pressure. (**a**) Contour plane of L and R factors; (**b**) response surface of L and R factors.

As shown in Figure 15a, the density of the contour line distribution of D is greater than R, indicating that D has a greater influence on the average rail pressure than R. As shown in Figure 15b, there is a significant change in the inclination of the surface in the direction of the D change, while the inclination of the surface in the direction of the R change is relatively small, indicating that D has a significant impact on the average rail pressure. The minimum rail pressure is distributed in the areas with a smaller D and R. The minimum rail pressure is distributed in the areas with a smaller D and R, which is the lower left position of the surface.

(a) (b)
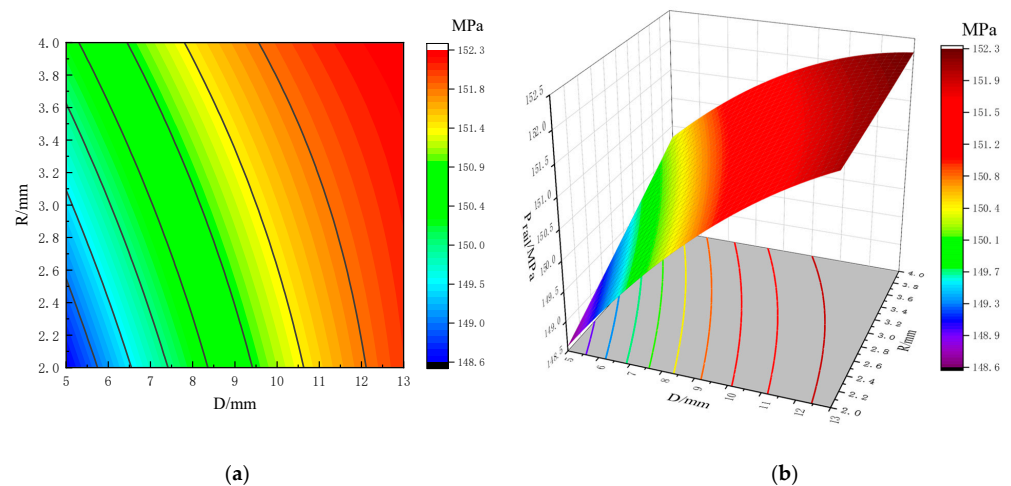
Figure 15. Interaction response of design variables D and R with average rail pressure. (**a**) Contour plots of D and R factors; (**b**) response surface of D and R factors.

5.4.2. Response Surface Optimization Analysis of the Average Rail Pressure Fluctuations ΔP in the Common Rail Pipe

As shown in the Figure 16a contour plane, the maximum rail pressure fluctuations occur at the position where D is smaller and L is smaller, and the density of the contour line distribution in the D direction is much greater than that in the L direction, indicating that D has a greater influence on rail pressure fluctuations than L. According to Figure 16b,

as L and D increase, the rail pressure fluctuations inside the common rail pipe show a downward trend. Moreover, the decrease in rail pressure in the D direction is much greater than the decrease in rail pressure in the L direction, which further verifies that the influence weight of D on the rail pressure fluctuations is greater than that of L.

(**a**)   (**b**)
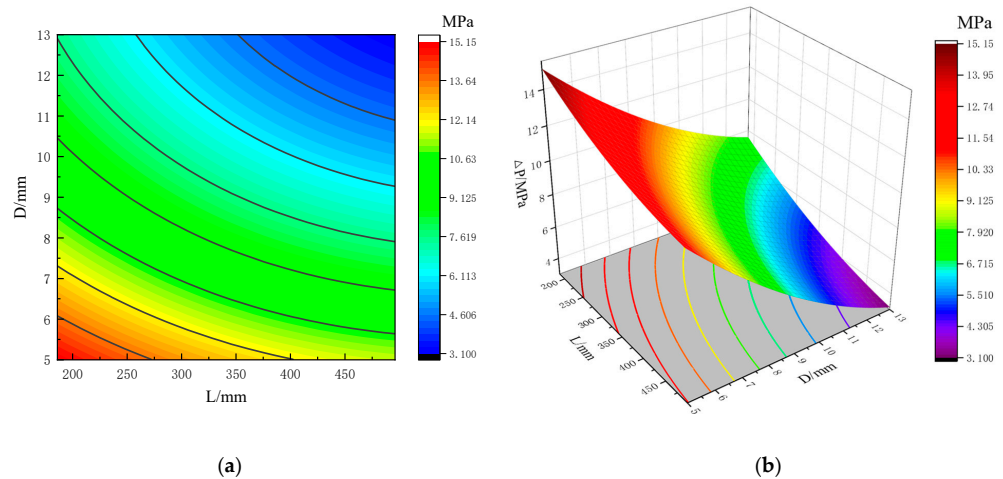
Figure 16. Interactive response of rail pressure fluctuations for design variables L and D. (**a**) Contour plane of L and D factors; (**b**) response surface of L and D factors.

As shown in Figure 17a contour plane, the density of the contour line in the L direction is greater than that of the contour line in the R direction, indicating that L has a greater influence on rail pressure fluctuations than R. As shown in Figure 17b, the minimum value of rail pressure fluctuations is located at the positions with a larger L and R, which is the lower left side of the response surface. The rail pressure fluctuation range in the L direction is about 5 MPa, and the rail pressure fluctuation range in the R direction is about 2 MPa.

(**a**)   (**b**)
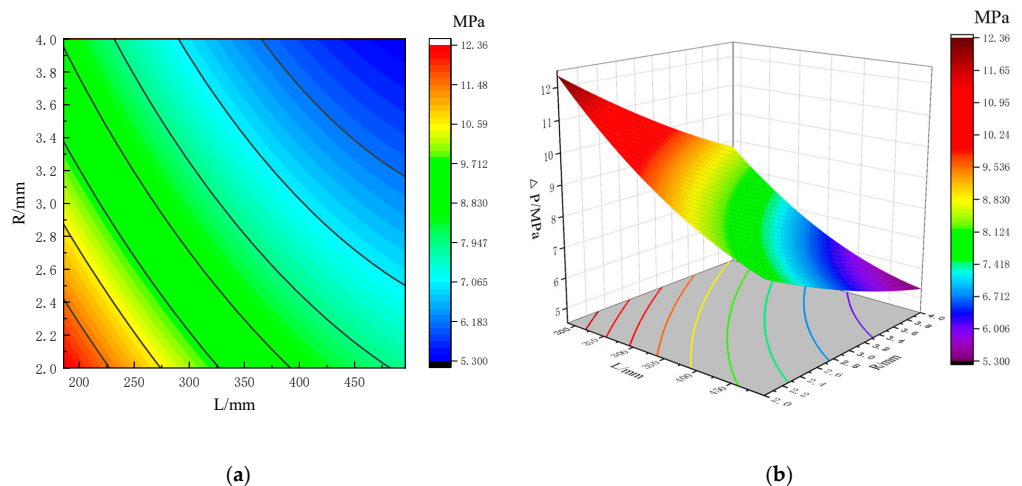
Figure 17. Interactive response of rail pressure fluctuations for design variables L and R. (**a**) Contour plane of L and R factors; (**b**) response surface of L and R factors.

As shown in Figure 18a contour plane, the density of the contour line in the D direction is much greater than the density of the contour line in the R direction. This is because the change in the size of D has a greater impact on the volume of the HPCRIS, indicating that D has a much greater impact on rail pressure fluctuations than R. As shown in Figure 18b, it can be seen that the surface in the D direction descends faster, further proving that D has a more significant impact on rail pressure fluctuations. The rail pressure fluctuations

decrease with the increase in *D* and *R*, and the minimum value of rail pressure fluctuations is distributed at the lower left side of the curved surface.

(**a**)   (**b**)
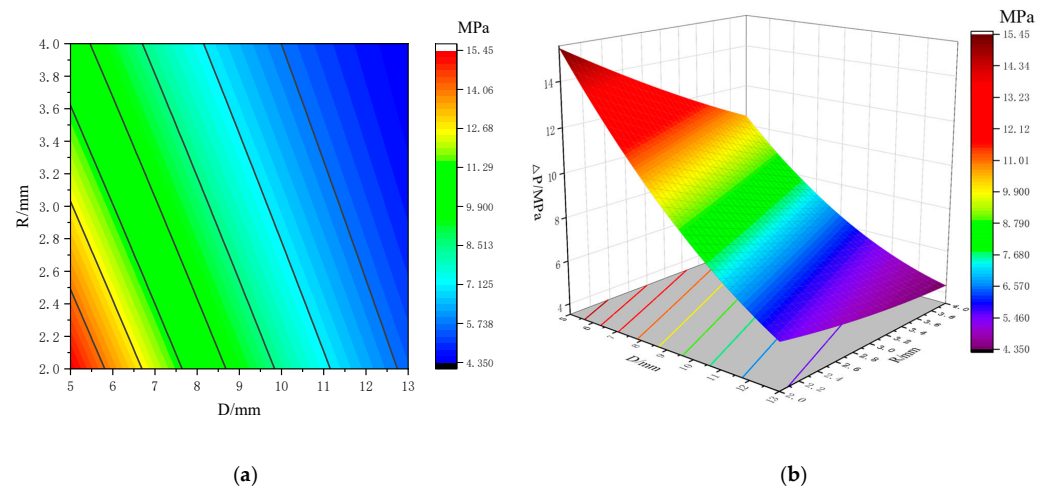
Figure 18. Interactive response of rail pressure fluctuations for design variables *D* and *R*. (**a**) Contour plane of *D* and *R* factors; (**b**) response surface of *D* and *R* factors.

For the polynomial regression model of the average rail pressure and average rail pressure fluctuations, the minimum value of the common rail pipe pressure fluctuations and the set value of common rail pipe pressure near 150 MPa are taken as the optimal values, and the optimal parameter combination of the regression model is solved and rounded. The optimal parameters obtained are *L* = 293.9 mm, *D* = 8.2 mm, *R* = 3.1 mm.

6. Test Verification of the HPCRIS for Diesel Engines

The test platform of the HPCRIS for diesel engines is shown in Figure 19. The test bench mainly consisted of a fuel tank, filter, low-pressure pump, high-pressure pump, overflow valve, common rail pipe, high-pressure fuel pipes, pressure gauge, controller, sensors, data acquisition device and display panel. It can conduct a flow characteristics test and pressure change characteristics test of the HPCRIS. The principle of the test platform is shown in Figure 20, where the pressure sensor was installed at the common rail pipe to collect data on the rail pressure signal, and the fuel flow sensors were installed at the outlet of fuel injectors to measure the volume of fuel injected by fuel injectors.

Figure 19. Test platform of the HPCRIS for diesel engines.
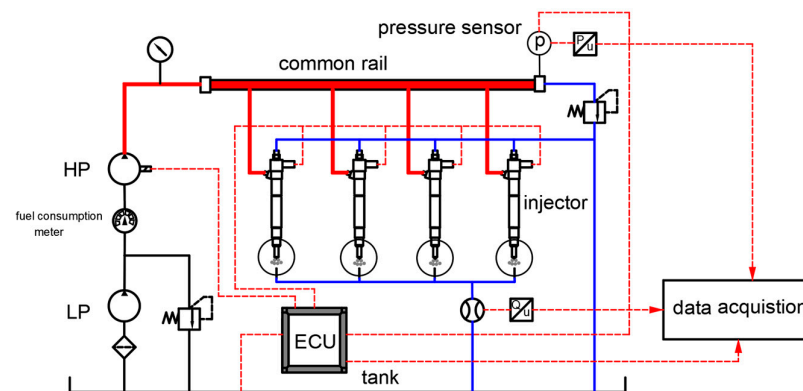
Figure 20. Hydraulic schematic diagram.

During the test, the test platform was started, and the diesel was pressurized by the low-pressure and high-pressure oil pumps before entering the high-pressure common rail pipe for pressure stabilization. Then, it entered the fuel injectors, where the high-pressure diesel was injected into the fuel collection device through the nozzle hole. Finally, the collected low-pressure pipeline flowed back into the fuel tank. During the experiment, the target rail pressure was set to 150 MPa on the test platform of the HPCRIS for diesel engines, setting the test time to 300 s, and conducting data collection when the system was in the stable voltage stage. By collecting signals from the pressure gauge and pressure sensors in the system, changes in pressure data inside the common rail pipe were obtained. After the experiment, the collected rail pressure curve data were imported into a computer for analysis and processing, in order to obtain specific values of fuel injection characteristic parameters, such as the average rail pressure and average rail pressure fluctuations during this experiment.

Under the working condition of the target rail pressure of 150 MPa, repeat tests were conducted on the common rail pipe and high-pressure fuel pipes of the HPCRIS used in diesel engines before and after optimization. To ensure the accuracy of the test results, this paper conducted 15 repeated tests on the average rail pressure, average rail pressure fluctuations, and other fuel injection characteristics data of a single test. The average value of the 15 measured data was taken to obtain the total average rail pressure, total average rail pressure fluctuations, total average fuel injection pressure, and total average fuel injection quantity of the fuel injector under this working condition. The fuel injection characteristics test data before optimization are shown in Table 8, and the fuel injection characteristics test data after optimization are shown in Table 9.

Table 8. Fuel injection characteristics test data before optimization.

Test Number	Average Rail Pressure before Optimization P_{rail}/MPa	Average Rail Pressure Fluctuations before Optimization ΔP/MPa	Average Injection Pressure before Optimization P/MPa	Average Fuel Injection before Optimization V/mm^3
1	149.71	11.92	142.73	64.83
2	149.61	12.33	142.35	64.92
3	149.69	11.94	142.43	64.72
4	149.93	11.85	142.56	64.76
5	149.68	11.42	141.97	64.58
6	149.63	11.65	142.42	64.31
7	149.54	11.64	142.58	65.16
8	149.65	12.25	142.82	64.82
9	149.52	11.95	142.65	64.67
10	149.64	11.64	142.14	64.72
11	149.78	11.08	142.48	64.68
12	149.15	12.23	141.95	64.89
13	149.63	12.38	142.67	64.62
14	149.58	11.31	142.34	64.55
15	149.56	12.26	142.35	64.87
Total average	149.62	11.86	142.43	64.74

Table 9. Fuel injection characteristics test data after optimization.

Test Number	Average Rail Pressure after Optimization P_{rail}/MPa	Average Rail Pressure Fluctuations after Optimization ΔP/MPa	Average Injection Pressure after Optimization P/MPa	Average Fuel Injection after Optimization V/mm^3
1	150.72	9.22	143.72	65.48
2	150.88	9.04	143.54	65.72
3	150.76	8.64	143.89	65.13
4	150.03	9.16	143.76	65.49
5	150.81	9.06	143.51	65.02
6	150.64	8.45	144.04	64.87
7	150.68	8.56	143.42	65.34
8	150.92	8.47	143.31	65.47
9	150.79	8.85	143.86	65.53
10	150.78	9.16	143.95	64.98
11	150.68	8.14	143.82	64.91
12	150.67	9.02	143.56	65.18
13	150.63	8.54	143.97	65.28
14	150.45	8.36	143.65	65.34
15	150.27	8.61	143.59	65.57
Total average	150.65	8.75	143.71	65.29

The simulation values and total average experimental values of the fuel injection characteristics of the HPCRIS for diesel engines before and after optimization are shown in Figure 21. Add the total average value of the test with error bars to the fuel injection characteristic test figure and, by comparing the values in this test with the simulation values, it is concluded that this improvement is reliable. The maximum error between the simulation value and the experimental value of the HPCRIS is 3.6%, and less than 5%, which means that the precision of the established simulation model is high and can be used to analyze and study the injection characteristics of the system. According to the simulation model data of the HPCRIS in Figure 21, the optimized common rail pipe pressure was increased by 1.22 MPa, and the average rail pressure was increased by 0.82%; the average pressure fluctuations were decreased by 2.48 MPa, and the rail pressure fluctuations were reduced by 21.66%; the injection pressure of fuel injectors was increased by 1.64 MPa, and the injection pressure was increased by 1.15%; the single injection volume was increased by 0.55 mm^3, and the single injection volume was increased by 0.85%; after optimization, the injection performance of the HPCRIS significantly improved.
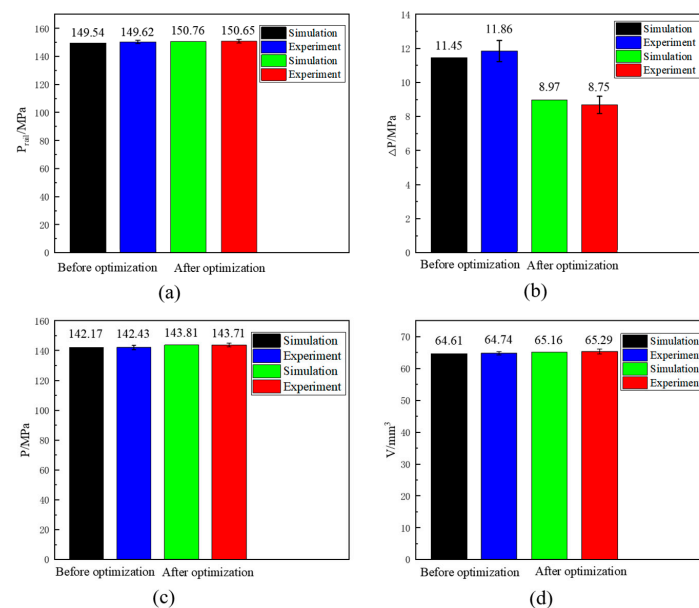
Figure 21. HPCRIS fuel injection characteristics before and after optimization. (**a**) Average rail pressure; (**b**) average rail pressure fluctuations; (**c**) average injection pressure; (**d**) average fuel injection volume.

7. Conclusions

In this paper, a simulation model of the diesel engine HPCRIS was established using AMESim 2020 simulation software, and the established model was tested and verified. Firstly, the influence of the key structural parameters of the common rail pipe and high-pressure fuel pipes on fuel injection characteristics was simulated and analyzed, and the influence laws of common rail pipe length *L*, common rail pipe diameter *D*, and high-pressure fuel pipe diameter *R* parameters on fuel injection characteristics were obtained. According to the structural parameters of the existing common rail pipe and high-pressure fuel pipes, a polynomial regression model of average rail pressure and pressure fluctuations in the common rail pipe was constructed by the response surface methodology. Based on this model, the structural parameters were optimized to minimize the pressure fluctuations in a common rail pipe and stabilize the average rail pressure near the set value. The relevant conclusions of this paper are as follows:

(1) The length *L* of the common rail pipe, the diameter *D* of the common rail pipe, the diameter *R* of high-pressure oil pipes, the product term *DR* of the common rail pipe diameter and the diameter of high-pressure oil pipes, as well as the square D^2 of the common rail pipe diameter, are all important influencing factors for the regression model under the average rail pressure and rail pressure fluctuations.

(2) When the diameter *D* of the common rail pipe and the diameter *R* of the high-pressure oil pipes remain unchanged, increasing the length *L* of the common rail pipe can increase the pressure on the common rail pipe and reduce the pressure fluctuations in the common rail pipe, but the slope of the curve change is relatively slow. When *L* and *R* remain constant, increasing *D* can effectively increase the average pressure on the common rail pipe and reduce the pressure fluctuations in the common rail pipe, further indicating that diameter *D* of the common rail pipe has a significant impact on the rail pressure and rail pressure fluctuations. When *L* and *D* remain constant, increasing the diameter of the high-pressure oil pipe can increase the common rail pressure and reduce the pressure fluctuations in the common rail pipe. However, with the continuous increase in *R*, the changes in the common rail pressure and common rail pressure fluctuations become more and more flat.

(3) Based on the average rail pressure and rail pressure fluctuation polynomial regression model of the HPCRIS used in diesel engines, with the minimum rail pressure fluctuations and the set value of the rail pressure system as the optimal objectives, the key structural parameters *L*, *D*, and *R* of the common rail pipe and the high-pressure fuel pipes were optimized by response surface methodology, and the optimal structural parameters of the common rail pipe and the high-pressure fuel pipes were obtained. After the optimization, the rail pressure of the HPCRIS was increased by 0.82%, the rail pressure fluctuations decreased by 21.66%, the injection pressure was increased by 1.15%, and the injection volume was increased by 0.85%, which further improved the injection performance of the HPCRIS for diesel engines.

Conflicts of Interest: The authors declare no conflict of interest.

References

1. Shi, M.W.; Wang, H.C.; Yang, C.L.; Wang, Y.Y.; Niu, X.X. Calibration and Prediction of Combustion Parameters Using Double-Wiebe Function Method Based on IMPSO. *Trans. CSICE* **2023**, *41*, 61–67.
2. Ou, S.H.; Yu, Y.H.; Dong, X.; Yang, J.G. Simulation and Experimental Investigation of Closed-Loop Combustion Control Strategy for Diesel Engines. *Trans. CSICE* **2023**, *41*, 211–219.
3. Yang, J.Y. Simulation Research on Combustion Process of Highly Intensified and Low Heat Dissipation Diesel Engine. Master's Thesis, Dalian University of Technology, Shanghai, China, 2022.
4. Mihyar, T.; Şen, E.; Soyhan, H.S. Impact of the JAZARI technology piston motion profile on the indicated thermal efficiency of a 4-cylinder diesel engine. *Fuel* **2023**, *351*, 128904. [CrossRef]
5. Wang, Y.H.; Wang, G.Y.; Yao, G.Z.; Shen, Q.Q.; Yu, X.; He, S.C. Combining GA-SVM and NSGA-III multi-objective optimization to reduce the emission and fuel consumption of high-pressure common-rail diesel engine. *Energy* **2023**, *278*, 127965. [CrossRef]
6. Gao, Z.G. Research on Injection Stability and Pressure Fluctuation of High-Pressure Common Rail System. Ph.D. Thesis, Beijing Jiaotong University, Beijing, China, 2022.
7. Zhao, T.B.; Wu, Y.S.; Duan, Y.Z.; Huang, Z.; Han, D. An experimental study on RP-3 jet fuel injection on a common rail injection system. *J. Cent. South Univ.* **2022**, *29*, 2179–2188. [CrossRef]
8. Fei, H.Z.; Qu, C.; Wei, Y.P.; Li, R.L. Simulation research on the prediction model of cyclic fuel-injection quantity for high-pressure common rail diesel engines. *J. Harbin Eng. Univ.* **2020**, *41*, 1651–1656.
9. Li, L.Y. Research on Fault Diagnosis of Diesel Engine High Pressure Common Rail System. Master's Thesis, North University of China, Taiyuan, China, 2022.
10. Wei, Y.P.; Fan, L.Y.; Chen, G.; Bai, Y.; Gu, Y.Q. Multiconfiguration fuel injection consistency of a high-pressure common rail system for a high-speed marine diesel engine. *J. Harbin Eng. Univ.* **2021**, *42*, 1330–1339.
11. Ge, J.C.; Yoon, S.K.; Song, J.H. Comparative Evaluation on Combustion and Emission Characteristics of a Diesel Engine Fueled with Crude Palm Oil Blends. *Appl. Sci.* **2021**, *11*, 11502. [CrossRef]
12. Wang, Z.Y. Study on the Simulation Research of High Pressure Common Rail Fuel Injection System of Diesel Engine Based on AMEsim. Master's Thesis, Chang'an University, Xian, China, 2017.
13. Li, Y.Q.; Wang, Y.P.; Chen, W.M.; Qiu, T.; Lei, Y.; Wang, J.E. Investigation of Rail Pressure Drop during Diesel Fuel Injection. *Trans. CSICE* **2022**, *40*, 263–269.
14. Nie, T.; Liu, Z.M.; An, S.J. Study of Pressure Fluctuation in the High Pressure Common Rail System. *Comput. Simul.* **2021**, *38*, 197–202.
15. Zhao, W.L. Simulation Research of Pressure Fluctuation in the Process of Fuel Supply and Injection for Common Rail System of Diesel Engine. Master's Thesis, Beijing Jiaotong University, Beijing, China, 2019.
16. Xiao, J.Y. Research on Injection Characteristics and Integrated Matching of Automotive High Pressure Common Rail System. Master's Thesis, North University of China, Taiyuan, China, 2021.
17. Wang, C.X. Simulation Research on Performance of Diesel Engine High Pressure Common Rail Fuel Injection. Master's Thesis, Jiangnan University, Wuxi, China, 2015.
18. Valeriy, K. Research on the Law of Pressure Fluctuation and Influencing Factors in the Fuel Rail of High-Pressure Common Rail Fuel System. Master's Thesis, Beijing University of Technology, Beijing, China, 2021.
19. Li, J.H.; Chen, H.L. Rail Pressure Control of Common rail Diesel Engine under Starting Condition. *Veh. Engine* **2019**, *244*, 57–62+68.
20. Feng, Z.Y. Design of Electronic Control of Diesel Engine Based on the Current Closed-Loop Control of Solenoid Valve. Master's Thesis, University of Electronic Science and Technology, Chengdu, China, 2018.
21. Li, R.L. Research on Fault Diagnosis Method of Abnormal Injection in Electronic Fuel System. Master's Thesis, Harbin Engineering University, Harbin, China, 2020.

22. Zheng, T. Research on Fault Diagnosis and Health Assessment of Injector in Common Rail System. Master's Thesis, Harbin Engineering University, Harbin, China, 2021.
23. Zhang, S.Z. Study on Transient Flow Characteristics of High Pressure Common Rail System. Master's Thesis, North University of China, Taiyuan, China, 2021.
24. Pu, Y. Research on the Observation Method of Fuel Injection Performance of High Pressure Common Rail System. Master's Thesis, North University of China, Taiyuan, China, 2023.
25. Lin, H.B. Research of High Pressure Common Rail Pipe Parameters on the Effects of Cavity Pressure Fluctuations. Master's Thesis, Chang'an University, Xi'an, China, 2017.
26. Zhu, L.J. Structural Optimization Design of High Pressure Common Rail Electronically Controlled Fuel Injection System for Diesel Engine. Master's Thesis, Hangzhou Dianzi University, Hangzhou, China, 2018.
27. Han, Y.H. Study on the Effect of Wear and Structure of Injector Needle Valve on Sealing Performance of High Pressure Common Rail System. Master's Thesis, North University of China, Taiyuan, China, 2023.
28. Wang, J.; Shen, L.Z.; Yang, Y.Z.; Bi, Y.H.; Wang, M.D. Optimal Calibration of Design Points of Off road Common rail Diesel Engine Based on Response surface methodology. *Trans. Chin. Soc. Agric. Eng.* **2017**, *33*, 31–39.
29. Chen, J.H. Optimization of Hydraulic Forming Process Parameters and Characteristics of Corrugated Pipe in Rocket Storage Tank. Master's Thesis, Yanshan University, Qinhuangdao, China, 2022.
30. Zhang, H.W. Fluid-structure Coupling Vibration Analysis and Parameter Optimization of Hydraulic U-shaped Hose. Master's Thesis, Guilin University of Technology, Guilin, China, 2021.
31. Gopal, K.; Sathiyagnanam, A.P.; Kumar, B.R.; Saravanan, S.; Rana, D.; Sethuramasamyraja, B. Prediction of emissions and performance of a diesel engine fueled with n-octanol/diesel blends using response surface methodology. *J. Clean. Prod.* **2018**, *184*, 423–439. [CrossRef]